

Supporting Information for

Unprecedented Li⁺ Exchange in an Anionic Metal–Organic Framework: Significantly Enhanced Gas Uptake Capacity

Bo Liu,^{†,‡} Rui Zhang,[‡] Chun-Yang Pan,^{*,†} and Hai-Long Jiang^{*,‡,⊥}

[†] School of Light Industry and Chemical Engineering, Guangdong University of Technology, Guangzhou 510006, China E-mail: panchuny@gdut.edu.cn

[‡] Hefei National Laboratory for Physical Sciences at the Microscale, Collaborative Innovation Center of Suzhou Nano Science and Technology, Department of Chemistry, University of Science and Technology of China, Hefei, Anhui 230026, P. R. China E-mail: jianglab@ustc.edu.cn

[⊥] State Key Laboratory of Structural Chemistry, Fujian Institute of Research on the Structure of Matter, Chinese Academy of Sciences, Fuzhou, Fujian 350002, P.R. China

Section 1 Materials and Instrumentation

All reagents and solvents were commercially available and were used without further purification. Infrared spectra were obtained in KBr discs on a Nicolet Avatar 360 FTIR spectrometer in the 400–4000 cm^{-1} region. Elemental analyses of C, H, and N were performed with a Perkin Elmer 2400C Elemental Analyzer. Thermalgravimetric analyses (TGA) were carried out in nitrogen stream using a Netzsch TG209F3 equipment at a heating rate of 5 $^{\circ}\text{C}/\text{min}$. Powder X-ray diffraction (PXRD) data were recorded on a Bruker D8 ADVANCE X-ray powder diffractometer ($\text{Cu K}\alpha$, 1.5418 \AA). Analyses for Li and Zn were carried out using an Optima 7300 DV inductively coupled plasma atomic emission spectrometer (ICP-AES). The sorption isotherms were measured with an automatic volumetric adsorption apparatus (Micrometrics ASAP 2020 M).

Section 2 Experimental Section

2.1 Synthesis of $[\text{H}_2\text{N}(\text{CH}_3)_2]_2[\text{Zn}_5(\text{L})_3]\cdot 5.5\text{DMF}\cdot 3.5\text{H}_2\text{O}$ (**1**)

A mixture of $\text{Zn}(\text{NO}_3)_2\cdot 6\text{H}_2\text{O}$ (0.029 g, 0.10 mmol), and H_4L (0.033 g, 0.10 mmol), dissolved in DMF 10 mL and placed in a Teflon-lined stainless steel vessel (25 mL), was heated at 130 °C for 72 h, and then cooled to room temperature at a rate of 3 °C min⁻¹. The resulting yellow block crystals of **1** were isolated by washing with DMF (5 mL×3) and dried in air (Yield: 52.2% based on H_4L). Anal. Calcd for $\text{C}_{68.5}\text{H}_{79.5}\text{N}_{7.5}\text{O}_{33}\text{Zn}_5$: C, 44.17; H, 4.30; N, 5.64. Found: C, 45.04; H, 3.91; N, 5.77. IR (cm⁻¹): 3445m, 3060w, 2931w, 2514w, 1793w, 1665s, 1624s, 1579s, 1412m, 1358s, 1310m, 1254w, 1176w, 1092m, 1023w, 907w, 829w, 778m, 724m, 662m.

2.2 Preparation of Li⁺-exchanged framework (**1-Li**)

Crystals of as-synthesized **1** were immersed in a saturated methanol solution of LiNO_3 for ten days, and the solution of LiNO_3 was refreshed daily. Upon decanting the solution, the cation-exchanged sample was rinsed with methanol and soaked in methanol for three days to remove residual LiNO_3 on MOF surface. The solid was filtered off and dried in air. Anal. Calcd for **1-Li** (After activation): C, 45.90; H, 1.61; N, 0.00. Found: C, 43.91; H, 2.30; N, 0.06. The big difference between the calcd and the found ones may be due to a small amount of water absorbed in the activation samples. IR (cm⁻¹): 3420m, 2499w, 1624s, 1578s, 1414m, 1359s, 1308m, 1178w, 1084m, 1017w, 902w, 828w, 768m, 723m, 698m, 662m.

Section 3 Crystallography

Diffraction data were collected at 296(2) with a Bruker-AXS SMART CCD area detector diffractometer using ω rotation scans with a scan width of 0.3° and Mo $K\alpha$ radiation ($\lambda = 0.71073 \text{ \AA}$). Absorption corrections were carried out utilizing SADABS routine. The structures were solved by direct methods and refined by full matrix least squares refinements based on F^2 with the SHELXTL program.¹ Non-H atoms were refined anisotropically with the hydrogen atoms added to their geometrically ideal positions and refined isotropically. The heavily disordered solvent molecules were trapped in the channels of **1** and **1-Li** could not be modeled properly. Thereby the SQUEEZE routine of PLATON² was applied to remove the contributions to the scattering from the guests. The final formulas of **1** and **1-Li** were determined by combining the single-crystal structures, elemental microanalyses and TGA data. Selected crystallographic data and structure refinement results are listed in Table S1.

References

- 1 Sheldrick, G. M. *SHELXL, version 6.12*; Bruker Analytical Instrumentation: Madison, WI, 2000.
- 2 Spek, A. L. *J. Appl. Crystallogr.* **2003**, *36*, 7–13.

Table S1. Crystallographic Data and Structural Refinement for 1 and 1-Li

	1	1-Li
Formula	C ₅₂ H ₃₄ N ₂ O ₂₄ Zn ₅	C ₄₈ H ₁₈ LiO ₂₄ Zn ₄
M_r	1397.66	1247.12
T (K)	296(2)	296(2)
cryst syst	Monoclinic	Monoclinic
space group	C2/c	C2/c
a (Å)	12.3215(10)	12.260(6)
b (Å)	30.711(3)	30.207(15)
c (Å)	22.7224(18)	22.980(11)
α (deg)	90	90
β (deg)	94.229(2)	94.983(10)
γ (deg)	90	90
V (Å ³)	8574.7(12)	8478(7)
Z	4	4
D_{calc} (g cm ⁻³)	1.083	0.977
$F(000)$	2808	2484
R_{int}	0.0681	0.0877
GOF on F^2	0.908	0.902
$R1^a$ [$I > 2\sigma(I)$]	0.0553	0.0562
wR2 ^b (all data)	0.1527	0.1548

$$^a R1 = \sum |F_o| - |F_c| / \sum |F_o|. \quad ^b wR2 = [\sum w(F_o^2 - F_c^2)^2 / \sum w(F_o^2)^2]^{1/2}.$$

Table. S2 Selected bond lengths (Å) and bond angles (deg) for **1**.

Zn(1)-O(8)#1	1.914(3)	Zn(2)-O(5)#3	1.911(3)
Zn(1)-O(10)	1.944(3)	Zn(2)-O(11)#4	1.941(3)
Zn(1)-O(4)#2	1.969(3)	Zn(2)-O(1)	1.946(3)
Zn(1)-O(2)	1.984(3)	Zn(2)-O(9)	1.990(3)
Zn(3)-O(3)#5	2.160(6)	Zn(3)-O(7)#6	2.254(4)
Zn(3)-O(3)	2.160(6)	Zn(3)-O(7)#7	2.254(4)
O(8)#1-Zn(1)-O(10)	122.84(16)	O(5)#3-Zn(2)-O(11)#4	114.34(16)
O(8)#1-Zn(1)-O(4)#2	120.62(16)	O(5)#3-Zn(2)-O(1)	125.57(16)
O(10)-Zn(1)-O(4)#2	110.48(17)	O(11)#4-Zn(2)-O(1)	106.50(15)
O(8)#1-Zn(1)-O(2)	100.55(18)	O(5)#3-Zn(2)-O(9)	99.11(15)
O(10)-Zn(1)-O(2)	101.52(16)	O(11)#4-Zn(2)-O(9)	95.31(14)
O(4)#2-Zn(1)-O(2)	92.06(16)	O(1)-Zn(2)-O(9)	111.57(14)
O(3)#5-Zn(3)-O(3)	135.5(5)	O(3)#5-Zn(3)-O(7)#6	91.38(18)
O(3)-Zn(3)-O(7)#6	96.96(16)	O(3)#5-Zn(3)-O(7)#7	96.96(16)
O(3)-Zn(3)-O(7)#7	91.38(18)	O(7)#6-Zn(3)-O(7)#7	157.9(4)

Symmetry codes: #1 -x+1, -y+2, -z+1; #2 -x+1, y, -z+3/2; #3 x+1, y, z; #4 -x+3/2, -y+3/2, -z+1; #5 -x, y, -z+3/2; #6 -x, -y+2, -z+1; #7 x, -y+2, z+1/2.

Table. S3 Selected bond lengths (Å) and bond angles (deg) for **1-Li**.

Zn(1)-O(8)#4	1.895(4)	Zn(2)-O(5)#6	1.902(4)
Zn(1)-O(10)	1.921(4)	Zn(2)-O(11)#7	1.938(3)
Zn(1)-O(4)#5	1.966(3)	Zn(2)-O(1)	1.973(4)
Zn(1)-O(2)	1.991(4)	Zn(2)-O(9)	1.986(3)
Li(1)-O(3)	1.933(7)	Li(1)-O(7)#2	2.005(8)
Li(1)-O(3)#1	1.933(7)	Li(1)-O(7)#3	2.005(8)
O(8)#4-Zn(1)-O(10)	119.33(18)	O(5)#6-Zn(2)-O(11)#7	115.65(18)
O(8)#4-Zn(1)-O(4)#5	115.05(16)	O(5)#6-Zn(2)-O(1)	121.04(18)
O(10)-Zn(1)-O(4)#5	112.44(15)	O(11)#7-Zn(2)-O(1)	108.46(16)
O(8)#4-Zn(1)-O(2)	104.63(17)	O(5)#6-Zn(2)-O(9)	101.13(16)
O(10)-Zn(1)-O(2)	108.29(16)	O(11)#7-Zn(2)-O(9)	95.03(15)
O(4)#5-Zn(1)-O(2)	93.03(16)	O(1)-Zn(2)-O(9)	112.13(15)
O(3)-Li(1)-O(3)#1	129.2(8)	O(3)-Li(1)-O(7)#2	100.10(17)
O(3)#1-Li(1)-O(7)#2	105.01(17)	O(3)-Li(1)-O(7)#3	105.01(17)
O(3)#1-Li(1)-O(7)#3	100.10(17)	O(7)#2-Li(1)-O(7)#3	119.1(7)

Symmetry codes: #1 -x+2, y, -z+1/2; #2 -x+2, -y+1, -z+1; #3 x, -y+1, z-1/2; #4 -x+1, -y+1, -z+1; #5 -x+1, y, -z+1/2; #6 x-1, y, z; #7 -x+1/2, -y+3/2, -z+1.

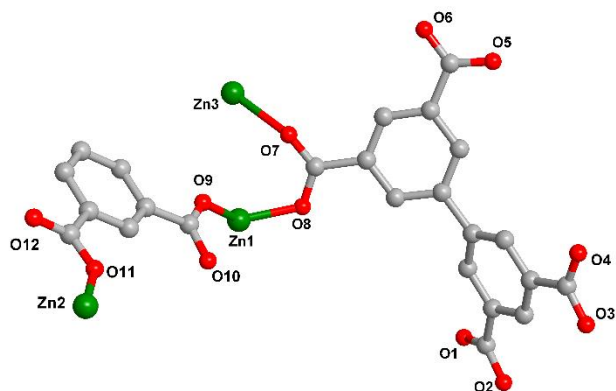
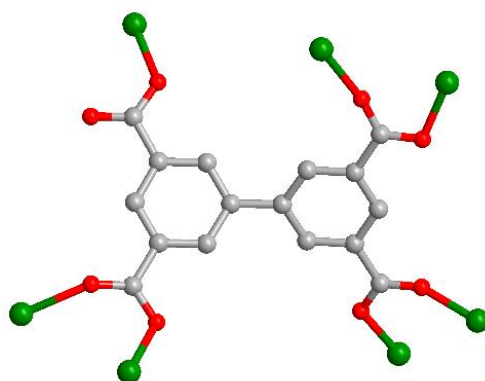
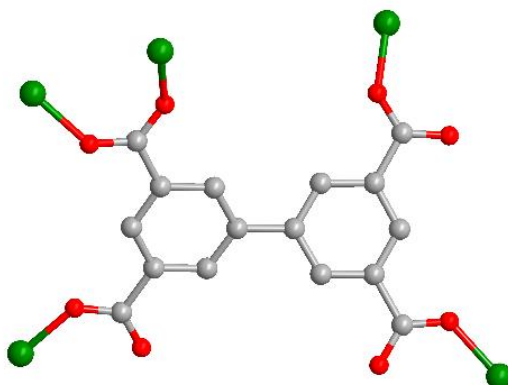


Figure S1. The coordination environment of Zn(II) in **1**.



(a)



(b)

Figure S2. Two kinds of bridging fashions of H₄L in **1**.

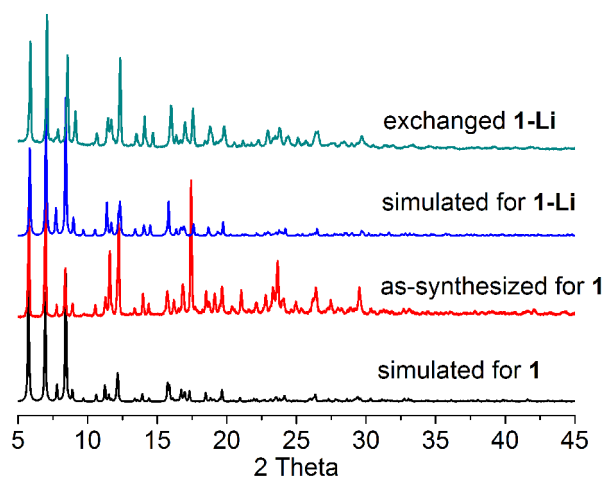


Figure S3. PXRD profiles of simulated and as-synthesized **1** and **1-Li**.

Section 4 Thermogravimetric analysis

Thermogravimetric (TG) analysis of **1** shows a significant weight loss of ~24.8 % in the range of 28-270 °C, which is attributed to the loss of guest DMF and H₂O molecules (calcd. 25.0%). Above 365 °C, a further heating induces decomposition of **1**. For **1-Li**, the first weight loss of about 12.9% within the temperature range 28-120 °C could be ascribed to the release of CH₃OH molecules (calcd. 13.0%). A weight loss of about 2.4% in the range 120-165 °C might correspond to the removal of H₂O molecules (calcd, 2.4%). After that, no further weight loss occurs before structural decomposition at 380 °C.

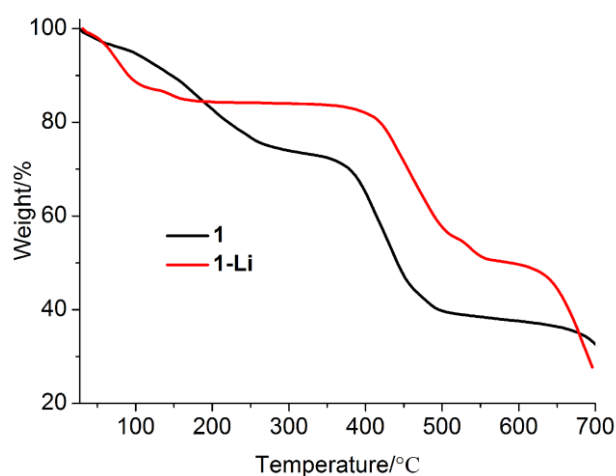


Figure S4. TGA plots for **1** and **1-Li**.

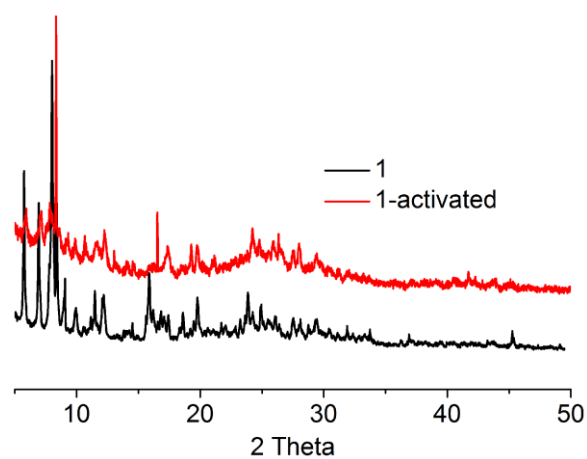


Figure S5. Experimental PXRD patterns for as-synthesized **1** and activated **1**.

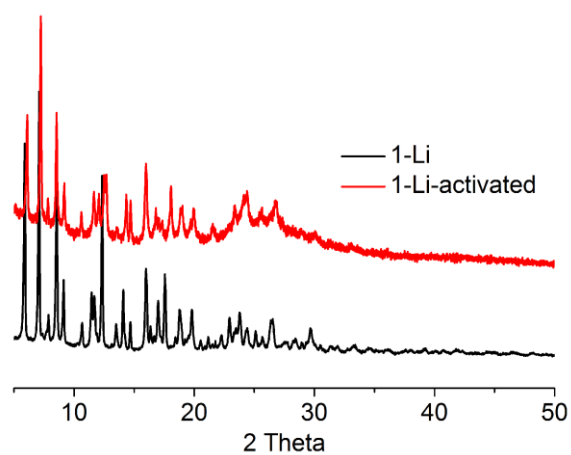
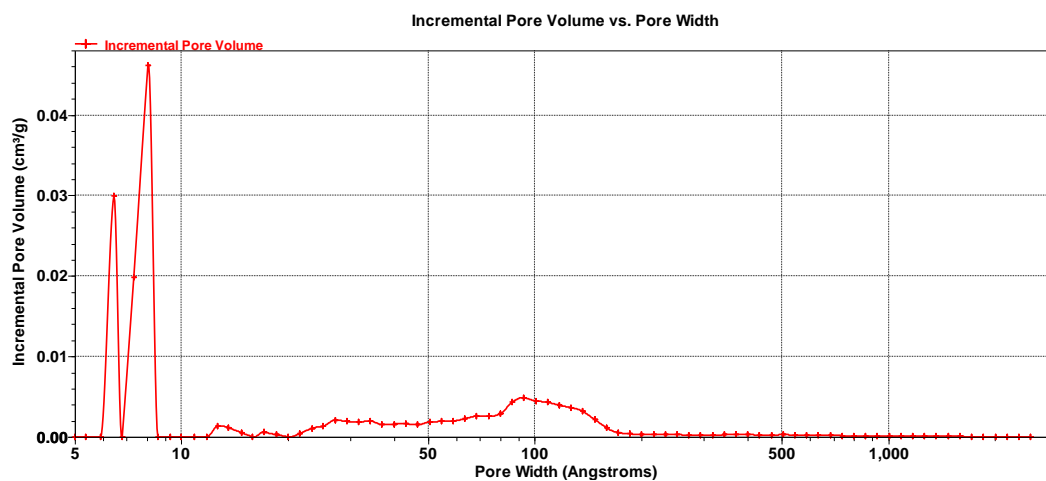
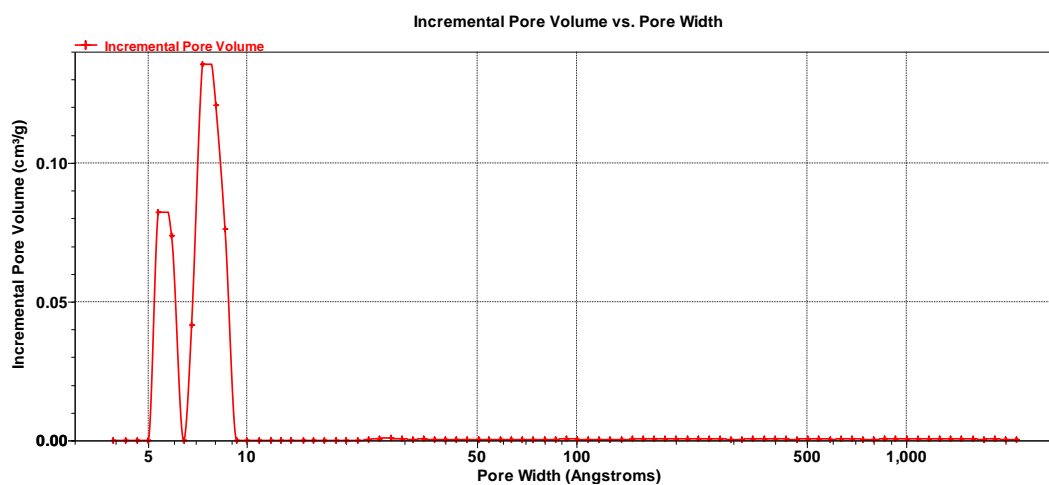


Figure S6. Experimental PXRD patterns for as-synthesized **1-Li** and activated **1-Li**.



(a)



(b)

Figure S7. Incremental pore volume as a function of pore width for **1** (a) and **1-Li** (b) calculated from the adsorption branch of 77 K N₂ using the Density Functional Model.

Section 5 IAST adsorption selectivity calculation:

The experimental isotherm data for pure CO₂ and CH₄ (measured at 298) were fitted using a Langmuir-Freundlich (L-F) model:

$$q = \frac{a * b * P^c}{1 + b * P^c}$$

Where q and p are adsorbed amounts and pressures of component i , respectively.

The adsorption selectivities for binary mixtures of CO₂/CH₄, defined by

$$S_{i/j} = \frac{x_i * y_j}{x_j * y_i}$$

were calculated using the Ideal Adsorption Solution Theory (IAST) of Myers and Prausnitz.

Where x_i is the mole fraction of component i in the adsorbed phase and y_i is the mole fraction of component i in the bulk.

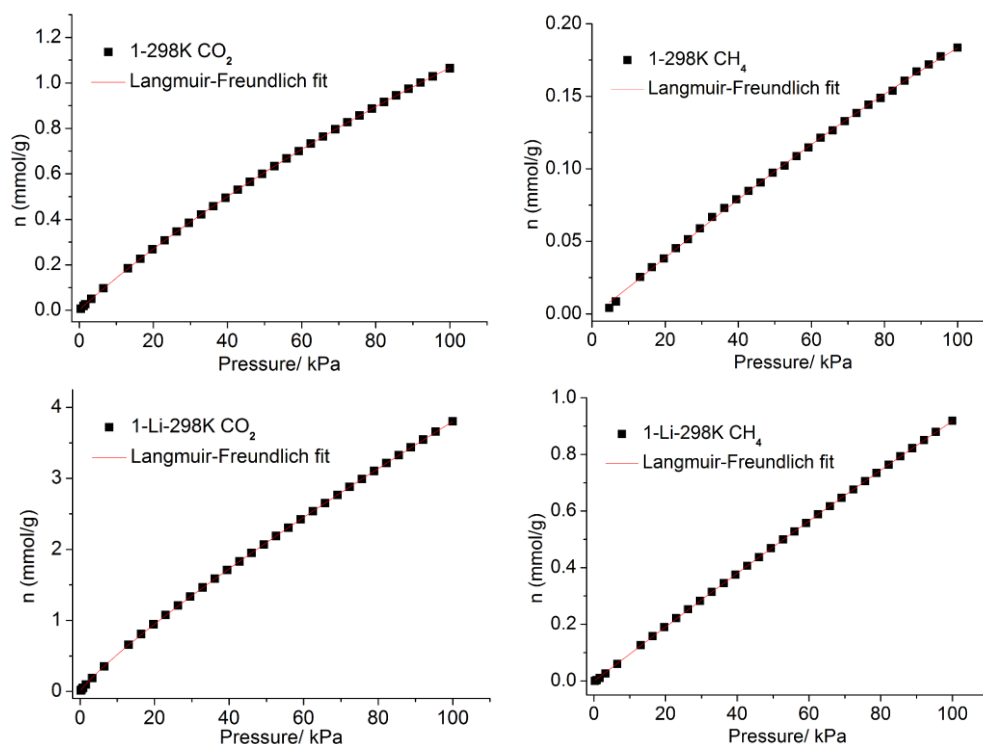
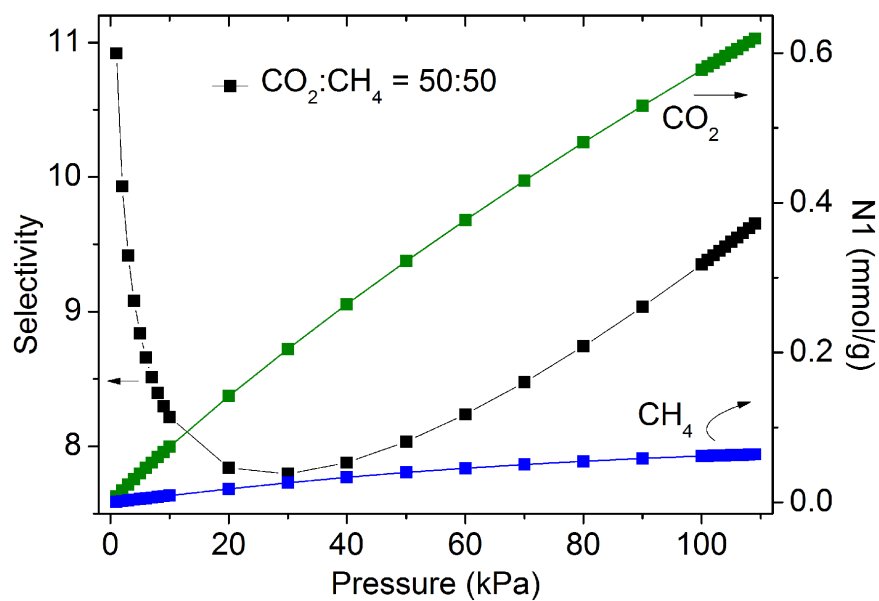
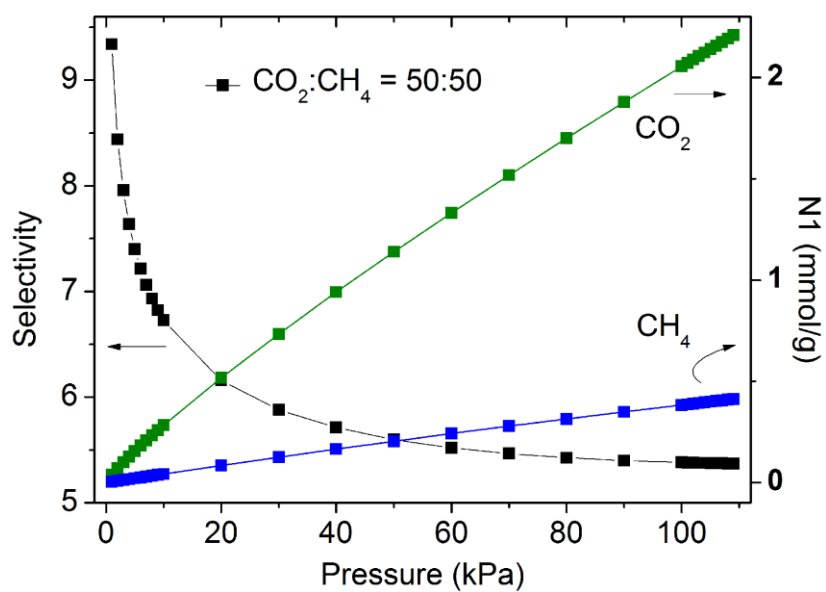


Figure S8. CO₂ adsorption isotherms of **1** with fitting by L-F model: $a = 5.46092$, $b = 0.00294$, $c = 0.95865$, $\chi^2 = 9.03 \times 10^{-7}$, $R^2 = 0.99999$; CH₄ adsorption isotherms of **1** with fitting by L-F model: $a = 0.70572$, $b = 0.00203$, $c = 1.11899$, $\chi^2 = 1.66 \times 10^{-6}$, $R^2 = 0.99941$; CO₂ adsorption isotherms of **1-Li** with fitting by L-F model: $a = 173.36595$, $b = 3.99981 \times 10^{-4}$, $c = 0.87426$, $\chi^2 = 3.20 \times 10^{-5}$, $R^2 = 0.99998$; CH₄ adsorption isotherms of **1-Li** with fitting by L-F model: $a = 9.96716$, $b = 9.05345 \times 10^{-4}$, $c = 1.0246$, $\chi^2 = 3.92 \times 10^{-6}$, $R^2 = 0.99995$.



(a)



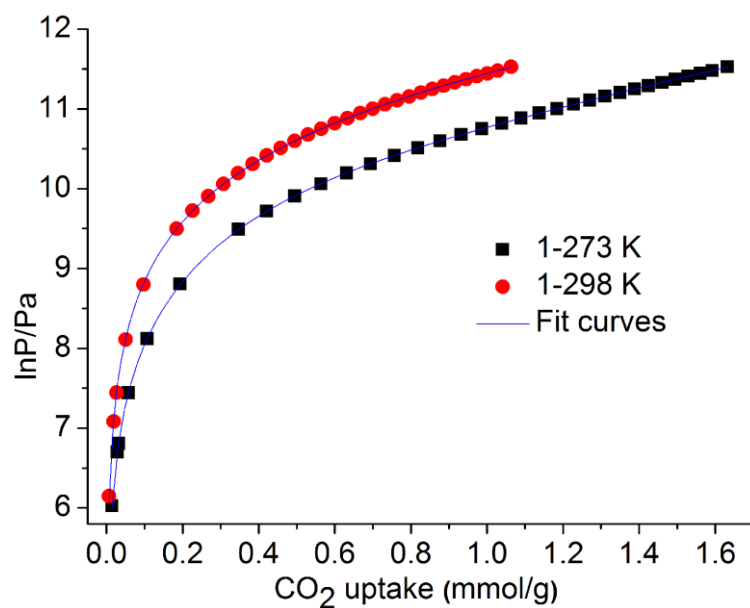
(b)

Figure S9. IAST adsorption selectivities of **1** (a) and **1-Li** (b) for equimolar mixtures of CO₂ and CH₄.

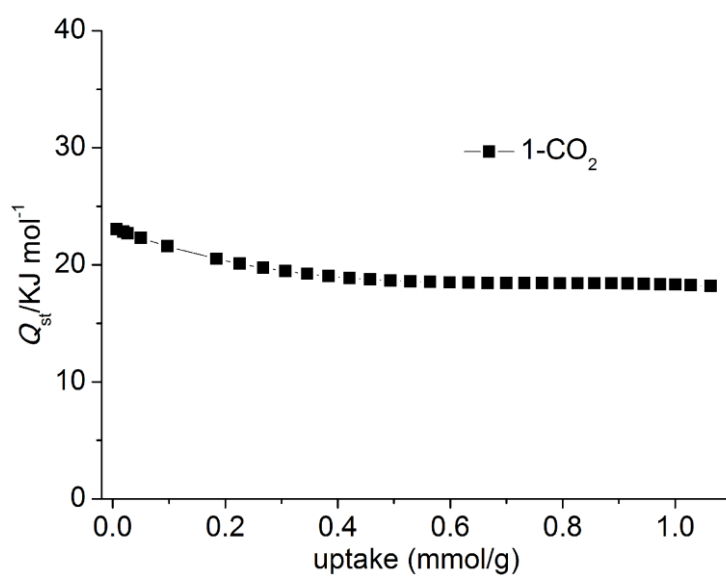
Section 6 Calculation of sorption heat for CO₂ uptake using Virial 2 model

$$\ln P = \ln N + 1/T \sum_{i=0}^m aiN^i + \sum_{i=0}^n biN^i \quad Q_{st} = -R \sum_{i=0}^m aiN^i$$

The above equation was applied to fit the combined CO₂ isotherm data for **1** and **1-Li** at 273 and 298 K, where P is the pressure, N is the adsorbed amount, T is the temperature, ai and bi are virial coefficients, and m and n are the number of coefficients used to describe the isotherms. Q_{st} is the coverage-dependent enthalpy of adsorption and R is the universal gas constant.

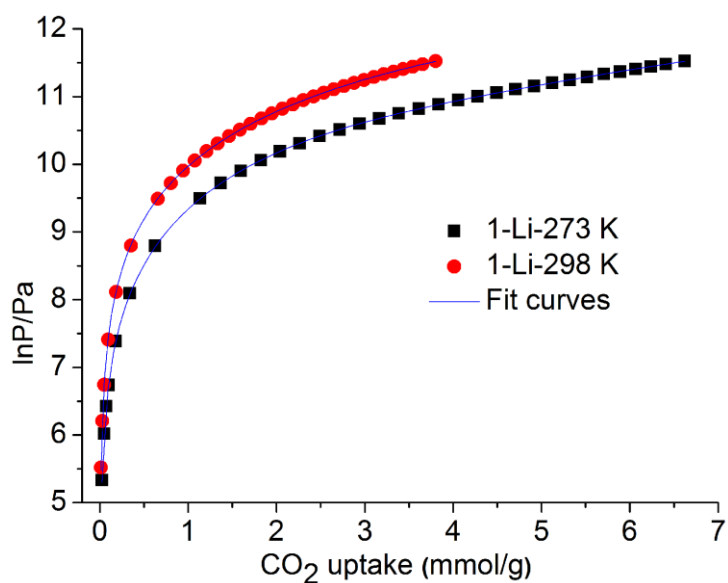


(a)

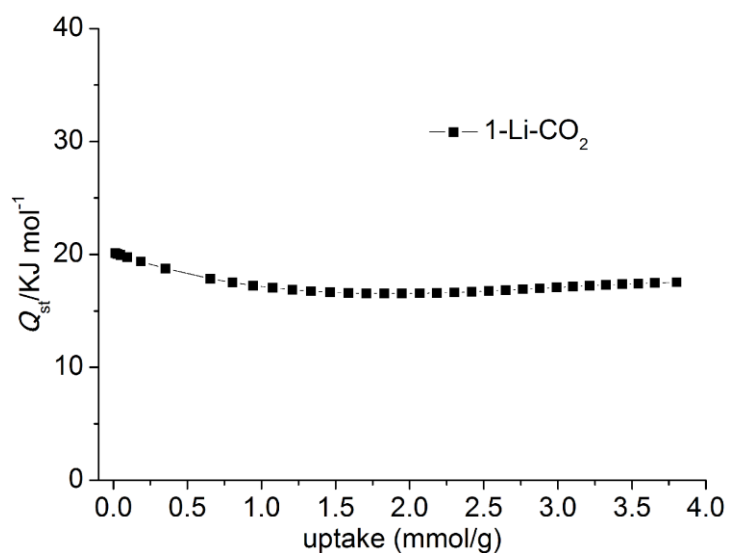


(b)

Figure S10. (a) CO₂ adsorption isotherms for **1** with fitting by Virial 2 model. Fitting results: $a_0 = -2785.16692$, $a_1 = 2232.43384$, $a_2 = -2971.99301$, $a_3 = 1391.65324$, $a_4 = -68.71331$, $b_0 = 20.42979$, $b_1 = -6.79223$, $b_2 = 9.15472$, $b_3 = -3.96077$, $\chi^2 = 1.71 \times 10^{-4}$, $R^2 = 0.99992$. (b) CO₂ adsorption heat calculated according to the virial equation.



(a)



(b)

Figure S11. (a) CO₂ adsorption isotherms for **1-Li** with fitting by Virial 2 model.

Fitting results: $a_0 = -2425.96285$, $a_1 = 559.00028$, $a_2 = -223.08388$, $a_3 = 26.84934$,

$a_4 = -0.28232$, $b_0 = 17.91019$, $b_1 = -1.61234$, $b_2 = 0.67578$, $b_3 = -0.07799$, $\text{Chi}^2 =$

8.40×10^{-5} , $R^2 = 0.99997$. (b) CO₂ adsorption heat calculated according to the virial

equation.